International Journal of Biological Macromolecules 164 (2020) 2051–2061

Contents lists available at ScienceDirect

International Journal of Biological Macromolecules

journal homepage: http://www.elsevier.com/locate/ijbiomac

NMR Relaxometry and magnetic resonance imaging as tools to determine the emulsifying characteristics of quince seed powder in emulsions and hydrogels

Irem Alacik Develioglu [a], Baris Ozel [a,b], Serpil Sahin [a], Mecit Halil Oztop [a,*]

[a] Middle East Technical University, Food Engineering Department, Ankara, Turkey
[b] Ahi Evran University, Food Engineering Department, Kirsehir, Turkey

ARTICLE INFO

Article history:
Received 29 February 2020
Received in revised form 8 August 2020
Accepted 9 August 2020
Available online 12 August 2020

Keywords:
Emulsion
Hydrogel
NMR Relaxometry
Magnetic resonance imaging
Quince seed
Xanthan gum

ABSTRACT

Quince seed powder (QSP) is known to exhibit emulsification properties and could be used as a natural emulsifier in colloidal food systems. In this study, emulsion-based alginate hydrogels were formulated using QSP and xanthan gum (XG) as stabilizers. The objective of the study was to show the emulsifying power of QSP in emulsions and their hydrogels using Time Domain (TD) NMR Relaxometry and Magnetic Resonance Imaging (MRI). Rheology and mean particle size measurements for emulsions and scanning electron microscope (SEM) experiments for hydrogels were further conducted as complementary methods. QSP containing emulsions were found to have longer T_2 relaxation times than XG samples ($p < 0.05$). Addition of either QSP or XG produced a more pseudoplastic flow behavior ($p < 0.05$) on the emulsions. Relaxation times were also obtained by MR images through T_2 maps. Relaxation decay curves showed the presence of two proton compartments in hydrogels; protons *associated with the polymer matrix* and *protons interacting with the oil phase*. The contribution of the first proton pools was the largest in QSP hydrogels confirmed by the lowest standard deviation in the T_2 maps. This behavior was explained by the emulsification ability of QSP. Results showed that NMR Relaxometry and MR images could be used to understand the emulsifying nature of QSP and many other hydrocolloids.

1. Introduction

Stabilization of oil in water emulsions is essential for many food products and this is usually achieved through stabilizers such as polysaccharides or emulsifiers or molecules that show both of these properties. In recent years, food scientists are continuously seeking ways to replace synthetic surfactants with natural alternatives to formulate '*green label*' products. Among these natural alternatives, food hydrocolloids such as xanthan (XG), pectin, alginate (AL), gum arabic have gained quiet high interest and have been studied extensively as alternative emulsifiers [1,2].

XG is a non-adsorbing complex polymer with high molecular weight and induces chain entanglements in water [3]. Thus, XG is mainly used as a thickening agent. Unique properties of XG enable to produce stable emulsions by increasing the viscosity of the continuous phase rather than adsorbing on the oil droplets [4].

Recently another hydrocolloid, extracted from the seeds *quince fruits* has also been studied by some researchers and shown to exhibit desirable properties in emulsions [5,6]. Quince seed powder (QSP) is extracted from the quince seeds and mainly comprises polysaccharides, cellulose and proteins [7]. QSP has been shown to possess surface activity on oil droplets and it was described as an adsorbing polymer [6].

Each biopolymer induces different surface activity and thickening characteristics in emulsions. Combination of various biopolymers is possible to manipulate the dispersion of the oil phase within the emulsion. Association of proteins and polysaccharides may provide amphiphilic complexes modifying both the rheology of the aqueous phase of the emulsions and the interfacial properties on the droplet surfaces [8].

Alginate (AL) is a linear anionic polysaccharide having L-guluronic and D-mannuronic acids as the major components [9]. In the presence of divalent ions (e.g., Ca^{2+}), carboxyl groups of guluronic acid units interact with these cations to form hydrogels [10]. AL is often used to modify emulsions, form hydrogels for drug delivery systems and produce edible films [9,11].

In this study; XG; QSP and alginate were used as biopolymers to formulate emulsions and emulsion hydrogels and the stability of these emulsions and hydrogels were assessed specifically by *NMR Relaxometry* and *Magnetic Resonance Imaging* (MRI) experiments.

NMR relaxometry is an important analytical tool that can be used for materials either in solid or liquid state. This technique is mostly based on measuring the relaxation times through different pulse sequences [12]. When a sample is placed in a magnetic field and exposed to a

* Corresponding author at: Middle East Technical University, Universiteler Mah. Dumlupinar Bulvari, No: 1 Cankaya, 06800 Ankara, Turkey.
E-mail address: mecit@metu.edu.tr (M.H. Oztop).

https://doi.org/10.1016/j.ijbiomac.2020.08.087
0141-8130/

radio frequency (rf) pulse; the spins are excited and once the rf pulse stops; spins relax back to their original position and generate the signal. From this signal, relaxation times are calculated. Relaxation times are intrinsic properties and show changes with the structural and physical changes in the systems. These relaxation times also known as spin-spin (T_2) and spin-lattice (T_1) relaxation times have been related with several physicochemical changes in food systems including gels [13–15]; emulsions [16–18]; confectionery products [19,20]. It can be used to determine pore size distribution in permeable media, water uptake, water/oil content and water distribution, adulteration [21–23], crystallization [16,24,25] in many different systems [26]. The information obtained from relaxometry comes from the whole samples and do not give localized information on the sample thus the data obtained are usually 1-dimensional. If the interest is to explore different regions in a sample Magnetic Resonance Imaging (MRI) can be used. MRI systems require magnetic gradient coils that can spatially gather the data. Therefore, creating two-dimensional and three-dimensional images that display areas having different physico-chemical properties (e.g., water content) with different contrasts becomes possible [27]. In MR images, the desired contrast is obtained by setting the proper acquisition parameters and the contrast depends on T_1 and T_2 times of the sample. Water uptake in hydrogels [28]; in vitro digestion of foods [29,30]; oil migration in chocolate [31,32]; drying of fruits [33] are just some examples that shows how MRI has been successfully used in food systems.

The objective of this study is to show the potential use of NMR Relaxometry and Magnetic Resonance Imaging (MRI) to differentiate emulsification characteristics of QSP and XG in an alginate hydrogel and on their corresponding emulsions. Rheology, particle size and SEM measurements were also conducted to complement NMR/MRI data and to confirm the findings of the method. The hypothesis of QSP acting on emulsions as an adsorbing polymer will have been confirmed in emulsions and emulsion hydrogels through relaxometry and MRI experiments.

2. Materials and methods

2.1. Materials

Alginate (AL), calcium chloride dihydrate ($CaCl_2.2H_2O$) and xanthan gum (XG) were supplied from Sigma-Aldrich Chemical Co. (St. Louis, MO, USA). Whey protein isolate (WPI) was purchased from Bipro Hardline Nutrition (Kavi Gıda San. Ltd. Sti., Istanbul). Sunflower oil (Yudum Gıda San. Tic. A.S., Ayvalik, Balikesir) was purchased from a local grocery store. Quince seed powder (QSP) was prepared by using the seeds of quinces purchased from a local supermarket in Ankara.

2.2. Quince seed powder preparation

Quince seeds were separated from the fruits, frozen and then dried using a freeze drier (Christ, Alpha 2–4 LD plus, Germany) for 48 h at −50 °0C and at 0.019 mbar [18]. Following drying, samples were ground to a powder form by using a coffee grinder (MC23200, Siemens, Germany).

2.3. Emulsion preparation

Formulation of the emulsions was determined with preliminary trials. Since alginate does not possess emulsification properties; WPI was added as an emulsifier to the mixture. Protein concentrations of 1–3% (*w*/w) are typically used in emulsions for stabilization since protein adsorption rate at these concentrations is not a limiting factor for emulsion formation [34]. To prepare the emulsions; 2% WPI, 2% AL, and 10% refined sunflower oil (all (*w*/w)) were dissolved in distilled water by using a high-speed homogenizer at 14,000 rpm for 4 min (IKA, Corp., Staufen, Germany). XG and QSP were added to the emulsions at a concentration of 0.5% (*w*/w) [6]. During the preparation of QSP containing emulsions, after all raw materials were homogenized for 1 min (WiseTisHG-15D, Wertheim, Germany), emulsion was centrifuged at 10,000 *g* for 2 min to remove the solid particles of seed powder. Then, centrifuged emulsion was re-homogenized at 14,000 rpm for 3 min.

2.4. Cold set gel preparation

As will be stated afterwards; MRI experiments were conducted for the hydrogels formulated in the study. Since a clinical MR scanner with a *'knee'* coil of 16 cm diameter was used, it is desired to make the gels as big as possible. For that purpose, gels were prepared using 50 mL of the prepared emulsions. Emulsions were denoted as Control (AL-WPI-Oil-Water), QSP (QSP-AL-WPI-Oil-Water) and XG (XG-AL-WPI-Oil-Water) and were put into 0.25 M [35] $CaCl_2$ solutions at a ratio of 1:3 by the help of plastic mesh baskets to enable isotropic diffusion. Gelation lasted for 18 h. All three emulsion types used for gelation contained AL, WPI and oil. Photos of hydrogels and plastic mesh baskets are shown in the *Supplementary document* (Fig. S1 and Fig. S2).

2.5. Mean particle size measurements

Mean particle sizes of emulsions were measured by using a light diffraction-based particle size analyzer (Mastersizer 3000, Malvern, Worcestershire, UK). Refractive index value was set to 1.56.

2.6. Scanning Electron microscopy experiments

Hydrogels were dried using a freeze dryer (Christ, Alpha 2–4 LD plus, Germany) for 48 h and then scanning electron microscopy experiments were performed using a Jeol electron microscope (JSM 6400, Tokyo, Japan) at 600 X magnification.

2.7. Rheological measurements

To complement the information that will be obtained through MRI and NMR experiments; rheological measurements were conducted on the three emulsion formulations (Control, QSP and XG) and on the XG and QSP polymer solutions using a cone-and-plate (40 mm diameter, 4° cone angle, and 0.1425 mm gap) rheometer (Kinexus Dynamic Rheometer, Malvern Instruments, Worcestershire, UK). Experiments were performed at 25 ± 0.1 °C. Flow curves were obtained from the experiments. For hydrogels, viscoelastic measurements were not conducted.

Rheological properties were determined at the concentration of 0.5% (*w*/w) for XG and QSP both for emulsions and for polymer solutions. For polymer solutions; flow curves were also obtained in the presence of $CaCl_2$ (*hydrocolloids were dissolved in 0.25 M $CaCl_2$ solution*) since gels were prepared with $CaCl_2$ as the crosslinking agent. Shear stress values were recorded with respect to varying shear rates data from 0.1 s^{-1} to 100 s^{-1} with 20 sample points and 2 min total ramp time. Data were fitted to the appropriate rheological model.

2.8. Nuclear magnetic resonance (NMR) Relaxometry measurements

NMR Relaxometry measurements were conducted both for the hydrogels and emulsion systems. In addition, to interpret the relaxation times better, T_2 measurements were also conducted for biopolymers and their combinations in different forms as will be explained later.

Spin-spin relaxation (T_2) measurements were conducted by using two different NMR spectrometers. *0.32 T* NMR spectrometer operating at 13.52 MHz ^{1}H-resonance frequency (Spin-Vision, Resonance System, Russia) was used for emulsion characterization. A Carr-Purcell-Meiboom-Gill (CPMG) pulse sequence was used with an echo time (TE) of 1000 μs, repetition time (TR) of 1000 ms, 16 acquisition points, and 64 scans to measure T_2 values. Since gels had shorter relaxation times, to have higher signal to noise ratios, their relaxation times were

acquired using a *0.5 T* (22.40 MHz) NMR spectrometer equipped with a 10 mm coil (SpinCore Inc., Gainesville, U.S.A). T_2 measurements with this instrument were also conducted using CPMG sequence with a TE of 1000 μs, TR of 3000 ms and 32 scans. Spin lattice relaxation times (T_1) were also measured for gels and inversion recovery (IR) pulse sequence was used for these measurements. Inversion times changed between 1 and 10 ms and repetition delay of 3 s was used.

The samples for NMR experiments were prepared by loading 3 mL of sample into 15 mm diameter cylindrical plexiglass tubes for the SpinVision system and by loading 15 mm height of hydrogel sample into a 10 mm diameter cylindrical glass tubes for the SpinCore system. All NMR experiments were performed at room temperature (25 °C).

T_2 experiments were replicated three times for each sample, and mean T_2 values were calculated using a mono-exponential model by using MATLAB (Mathworks Inc., U.S.A). Multi-exponential behavior of the decay curves was also examined using XPFit (Soft Scientific, Alango, Israel). Representative XPFit outputs (*relaxation spectrum*) are also given in Fig. 1. Colored lines in the spectrum denotes a '*proton population*' with a distinctive T_2 value.

2.9. Magnetic resonance imaging experiments for hydrogels

MR images of hydrogels were acquired using a 3 Tesla clinical MR Scanner (SIEMENS, Germany). A knee coil of 16 cm diameter was used for the measurements. Multi Slice Multi Echo (MSME) sequence that was based on Spin Echo (SE) sequence was used to obtain the T_2 maps of the gels. TR of 3150 ms, TE of 13.8 ms were used with 32 echoes and 4 scans. A field of view (FOV) of 150 mm and matrix size of 128*128 were used. Slice thickness was set to 3 mm and among the seven slices obtained, the 4th slice (the middle one) was only used for the analysis. In each measurement, three gels of the same hydrocolloid and a control sample was used. Oil in a 10 mm tube and in a UV-cuvette were used as the reference samples to correct the hardware related signal intensity

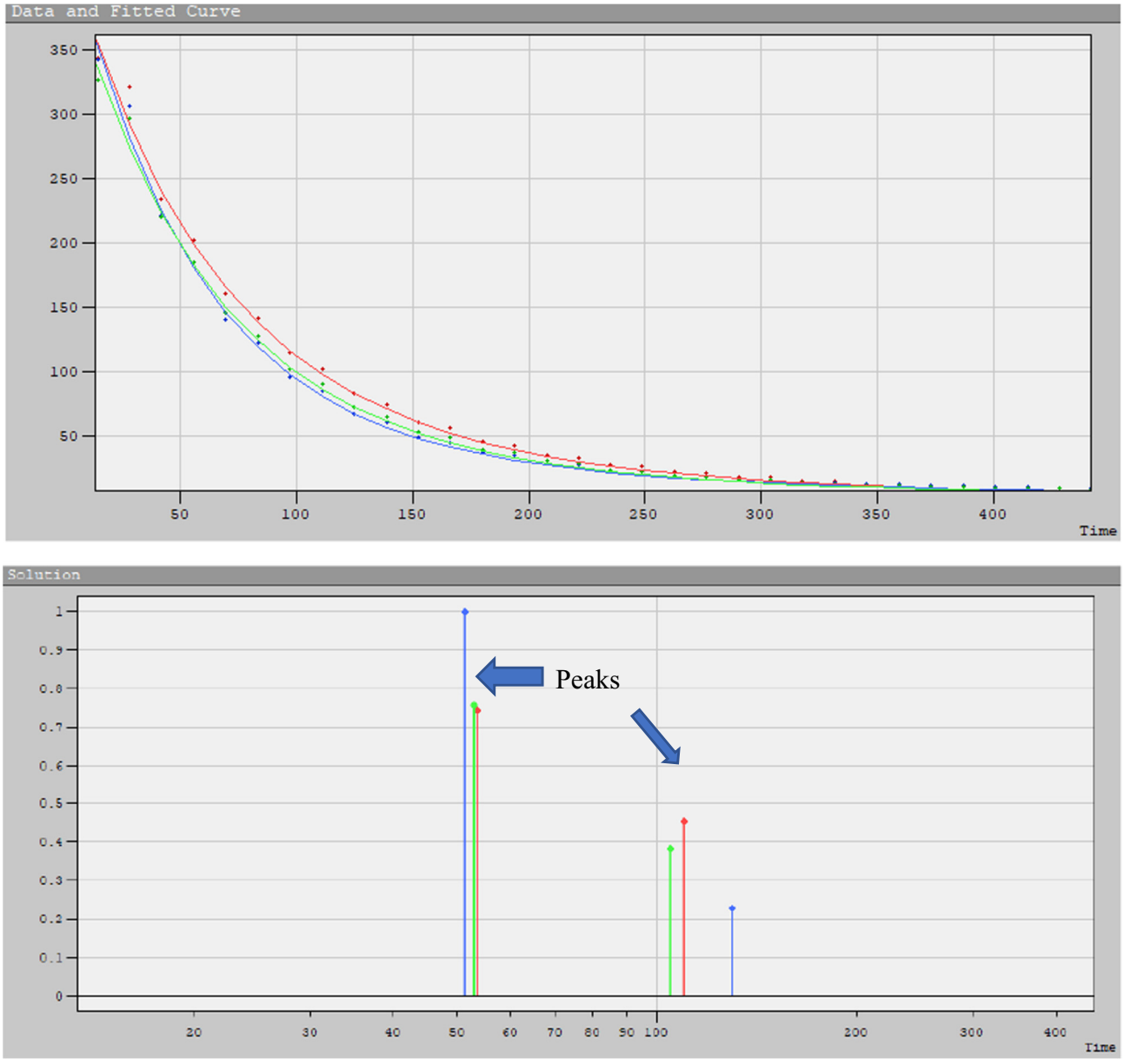

Fig. 1. *. Representative CPMG decay and XPfit relaxation spectra of the hydrogels. *XPfit display different compartments as lines not in the form of peaks as in other multi exponential relaxation analysis software.

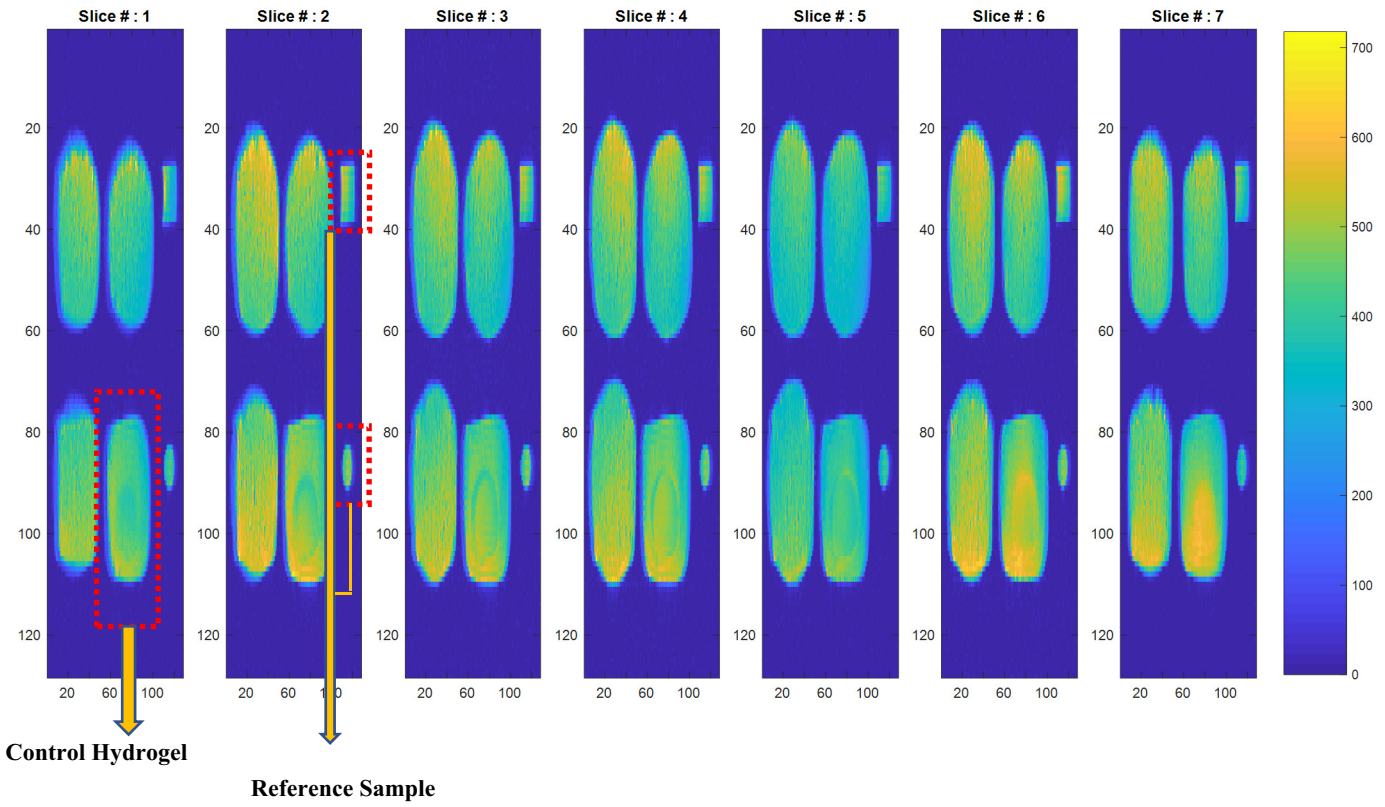

Fig. 2. *. Coronal (*Top view*) Spin Echo MR Images showing all 7 slices for quince seed including hydrogels (Slice Thickness of 5 mm, TE = 12 ms, TR = 3 s). *The bottom right gel in each slice (in red rectangle) corresponds to the 'Control Gel' (gel that does not include any hydrocolloid) and the rest are the 3 replicates of the same formulation. To account for instrument-based errors on signal intensity, sun flower oil (assuming that its signal properties not changing so signal intensity is constant) in a 10 mm tube (bottom right) and in a UV Cuvette (top-right) were also imaged. Axes of the images denotes the voxels as for the images 128*128 matrix size was used.

differences if needed. Representative MR images are provided in Fig. 2. For each gel, 3 replicates were analyzed as explained in the Fig.

Using the region of interest (ROI) tool of MATLAB, the gel region was selected and T_2 relaxation maps were obtained. T_2 maps of the selected region for different hydrocolloids and the control hydrogels were obtained by fitting the decaying signal to a mono exponential model. A T_2 map gives the spatial distribution of T_2 values in the gel. Thus, the standard deviation of a T_2 map image could give idea about the homogeneity of the sample. An example T_2 map is given Fig. 3.

In addition to T_2 maps, T_2 CPMG decay curves obtained from MSME images were further analyzed with XPFit to check the presence of different compartments and 2 compartments were detected in contrast to the experiments conducted at low magnetic field.

2.10. Statistical analysis

MINITAB (Version 16.2.0.0, Minitab Inc., State College, Penn, USA) was used for statistical analysis. All experimental results were analyzed by Analysis of Variance (ANOVA) Tukey's test at 5% significance level as the comparison test ($p < 0.05$). Comparisons were conducted to observe the effect of XG and QSP on results. At least three independent replicates were recorded for each sample.

3. Results and discussion

3.1. Particle size measurements

XG emulsions including AL and WPI as additional polymers, were shown to have the lowest particle size values with respect to Control and QSP emulsions which had the same composition (Fig. 4) ($p < 0.05$). The main reason behind this finding was the viscosity increasing effect of XG on the continuous phase. WPI molecules adsorbed onto the oil droplet surfaces and lowered the interfacial tension. Subsequently, these droplets fractured giving smaller diameter droplets. Later, small droplets were not able to coalesce again due to presence of XG and AL in the continuous phase. Thickening effect of XG and high hydrophilicity of AL molecules created a barrier for these droplets to come together thus, XG emulsions possessed the lowest particle size distribution ($p < 0.05$). At 0.5% (*w*/w) concentration, XG concentration was high enough to immobilize the oil droplets [3]. On the other hand, presence of only QSP could not retard oil droplet coalescence since QSP has a dominant interfacial activity rather than thickening effect. Both WPI and QSP had similar activity on the droplets and this did not cause a synergistic effect on lowering the mean particle size of the emulsions. Here, importance of the type of the polymer composition was justified. Control emulsions with no XG or QSP had the highest droplet size as expected ($p < 0.05$).

3.2. Rheological measurements

3.2.1. Polysaccharide solution rheology

Alginate is commonly used with Ca^{+2} to make hydrogels or gel beads [35–38]. In this study, hydrogels were also prepared from alginate and $CaCl_2$ and polysaccharides of XG and QSP were added to make the gels more stable. To interpret the effect of polysaccharides on the gel structure better; understanding the effect of Ca^{+2} cations, particularly on QSP was important. For this purpose, XG and QSP solutions were prepared with distilled water and $CaCl_2$ and the effect was analyzed via rheological measurements. Results are shown in Table 1. All solutions showed a Power Law behavior ($R^2 > 0.96$).

Effect of $CaCl_2$ on QSP and XG was different. Addition of $CaCl_2$ to XG solutions increased the consistency coefficient (k values) ($p < 0.05$). In

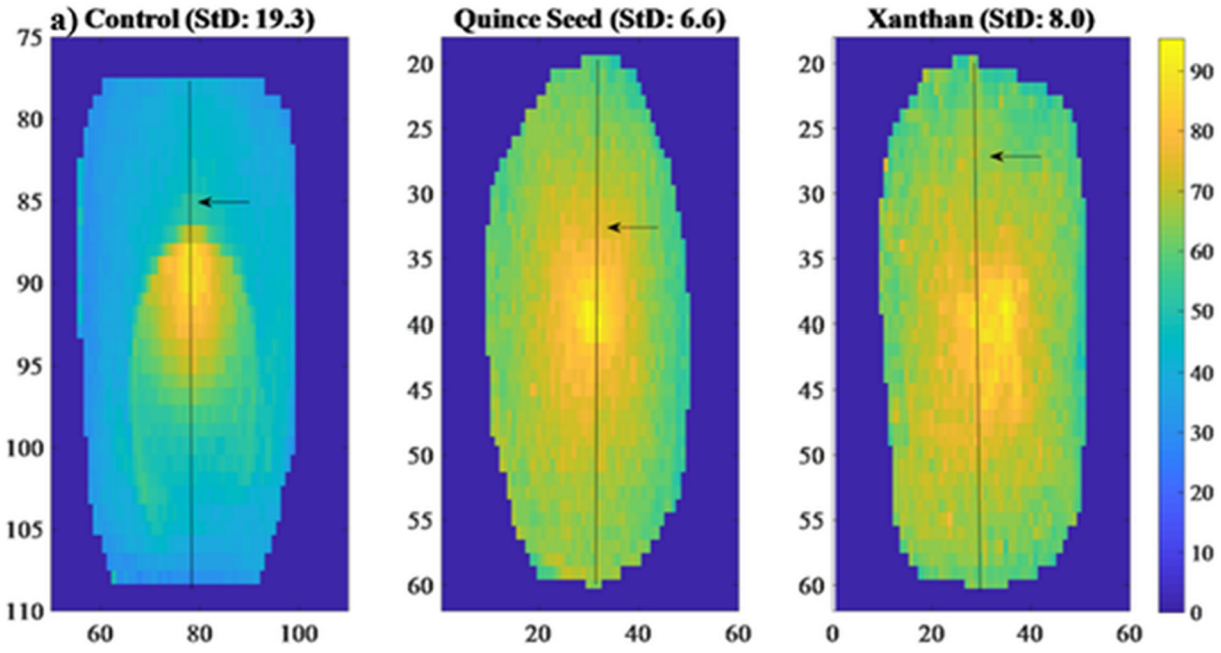

Fig. 3. T_2 maps of the *Control, QSP and XG* gels. Standard deviations of the T_2 values (calculated as the standard deviation of the all voxels in the 128*128 image) are shown in the title of the images indicating the heterogeneity/homogeneity in the gels.

contrast, Ca^{2+} ions did not result in higher viscosity for QSP solutions. 0.25 M Ca^{2+} ion concentration was more effective on XG due to the anionic and highly branched side chains of XG. Crosslinking density within the XG molecules could increase with $CaCl_2$ addition [39]. QSP, on the other hand, possesses a more linear structure [7] and this might have reduced the susceptibility of QSP molecules to Ca^{2+} action. Although QSP is an anionic polysaccharide, most charges are accumulated on the main backbone of the molecule [40]. Even after crosslinking with the added ion, conformation of the QSP molecules did not change sufficiently to alter the consistency index.

When flow behavior indexes were examined, both QSP and XG solutions were shown to experience shear-thinning character before and after $CaCl_2$ addition (n ~ 0.14–0.35) and XG samples had higher 'n' values compared to QSP.

XG solutions showed significantly higher 'n' values in 0.25 M $CaCl_2$ solution with respect to their correspondent solutions in distilled water ($p < 0.05$). The reason could be the contraction of the XG molecule because of the interactions between the side chains and the main cellulosic backbone. Ca^{+2} ions promoted crosslinking between the side chains of XG but also induced collapse of some side chains on the main XG cellulosic backbone [41]. Decrease of the hydrodynamic volume of the individual XG chains could have ended up with a higher n value ($p < 0.05$) [42].

QSP with less branched structure compared to XG [18], was more prone to exert a shear-thinning flow character with increasing shear rates ($n_{QSP} < n_{XG}$) whereas effect of $CaCl_2$ addition on QSP was reverse. $CaCl_2$ addition decreased the 'n' values significantly ($p < 0.05$). Intermolecular crosslinking effect of Ca^{2+} ions could have made it possible for QSP molecules to align in the direction of applied shear and resulted in smaller n values.

Besides the effect of Ca^{+2} ions on molecular conformations, XG and QSP solutions showed a consistent trend in rheological measurements. XG solutions always had higher viscosity and a more pseudoplastic flow behavior with respect to QSP solutions, regardless of the presence of $CaCl_2$. This consistency confirmed the characteristic differences of the respective polymers in terms of molecular conformation in the solutions. Consequently, consistency and flow behavior index results of XG and QSP polymers in the presence and absence of a cation demonstrated that each polymer had distinct flow characteristics and was affected differently form the presence of $CaCl_2$.

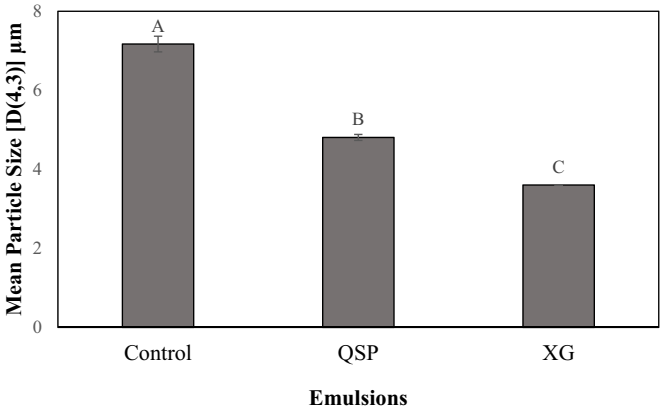

Fig. 4. Mean particle size [D (4,3)] values of emulsions ($p < 0.05$). Control, QSP and XG emulsions represent the formulations; AL-WPI-Oil-Water, QSP-AL-WPI-Oil-Water, XG-AL-WPI-Oil-Water, respectively. Error bars are represented as standard errors.

3.2.2. Emulsion rheology

Sun et al. (2007) reported that in the absence or presence of low amount of XG (0–0.02 *w*/w, %), 2% (*w*/w) WPI containing emulsions, these systems possessed Newtonian flow characteristics. At relatively higher XG concentrations (≥ 0.05 w/w, %) samples exhibited a shear-

Table 1
Rheological constants of polysaccharide solutions prepared by distilled water and 0.25 M calcium chloride solution. Different letters in each column mean solution type differed significantly ($p < 0.05$). Errors are represented as standard deviations. *

Solution	k (Pa.s^n)	n	R^2
XG-H_2O	20.41 ± 0.26^b	0.14 ± 0.01^b	0.989
XG-$CaCl_2$	63.44 ± 2.32^a	0.19 ± 0.01^a	0.965
QSP-H_2O	0.72 ± 0.11^B	0.35 ± 0.02^A	0.979
QSP-$CaCl_2$	1.04 ± 0.03^A	0.24 ± 0.01^B	0.989

* ANOVA was conducted for QSP and XG separately as the difference between 2 hydrocolloids was too large.

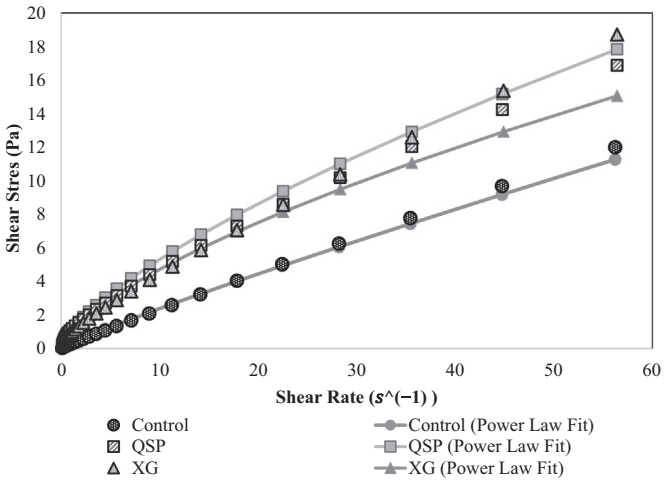

Fig. 5. Shear stress vs shear rate measurements and power law fitting curves of Control, QSP and XG emulsions.

thinning flow behavior as seen in Fig. 5. At higher shear rates, all samples also experienced a shear thinning effect. The reason was the more ordered alignment of the emulsion droplets along the flow direction at higher shear rates. XG emulsions attained *n* values less than unity and showed a decreasing trend with increasing XG concentration, suggesting a more pronounced shear-thinning behavior [3]. Therefore, the *n* value of XG emulsions found in our study was consistent with the previous results (Table 2). Compared to Control emulsions, both XG and QSP emulsions attained lower *n* values showing the increased shear thinning character of these samples ($p < 0.05$). XG or QSP addition also increased the *k* values of the emulsions demonstrating the higher viscosity of the gum added emulsions ($p < 0.05$).

Emulsion rheology results showed that addition of gum altered the rheology of the emulsions and the effects were similar. Although both XG and QSP emulsions attained similar *k* and *n* values, their stabilizing effects were different from each other. Bryant and McClements (2000) stated that 8.5% WPI and 0.2% XG (*w*/w) were thermodynamically compatible since their mixture solutions at pH 7.0 did not show any phase separation over a 72 h period [43]. They also suggested that XG dominated the rheological behaviors of these solutions. WPI – XG containing solutions were reported to achieve a much higher viscosity than only WPI or XG containing solutions. This synergistic effect was attributed to the conformation of WPI and XG molecules in the solution. The free volume available to XG molecules decreased by the presence of WPI and this increased the effective volume of the XG in the aqueous phase [44]. Therefore, increasing viscosity effect of XG was more consistent and XG produced thick non-adsorbing layers in contrast to QSP emulsions which was justified by the particle size measurements. QSP has shear thinning property like XG and it also has a high intrinsic viscosity leading to high hydrodynamic volume in solutions [45]. However, higher surface activity of QSP than XG resulted in a lower '*viscosity increasing effect*' for QSP in the emulsions.

3.3. NMR Relaxometry measurements

3.3.1. Transverse relaxation results

3.3.1.1. Polymer solutions and emulsions. Transverse relaxation which is also known as spin – spin relaxation (T_2) measures the relaxation rate of the ^1H protons in the transverse plane and depends on the efficiency of energy transfer between neighboring spins [12]. At first T_2 values were expressed as 'mono exponential 'and the effect of ingredients were discussed based on mono-exponential T_2 relaxation times. As will be seen in the latter section, multi compartmental analysis was also conducted on the emulsion relaxation data.

Table 2
Rheological constants of emulsions. Control, QSP and XG emulsions represent the formulations; AL-WPI-Oil-Water, QSP-AL-WPI-Oil-Water, XG-AL-WPI-Oil-Water, respectively. Different letters in each column mean emulsion type differed significantly ($p < 0.05$). Errors are represented as standard deviations.

Emulsion	k (Pa.s^n)	n	R^2
Control	0.31 ± 0.04^b	0.88 ± 0.03^a	0.999
QSP	1.04 ± 0.05^a	0.68 ± 0.02^b	0.997
XG	0.99 ± 0.02^a	0.68 ± 0.02^b	0.993

T_2 measurements of the polymer solutions and emulsions (Fig. 6) showed that QSP containing ones had longer T_2 times compared to XG containing ones except for WPI added gum solutions ($p < 0.05$). Another trend was the shorter T_2 of samples including oil which was an expected case since oil protons possess a higher rate of energy exchange rate compared to water protons [6,27].

Longer T_2 times of QSP-water compared to XG-water solution was mainly due to the big and complex structure of XG molecules. Side chains of XG interacted more intensely with the surrounding water molecules giving shorter T_2 times [46]. Particularly, viscosity increasing effect of XG molecule originating from its helical conformation in water also decreased the mobility of water and shortened the overall T_2 times. Amphiphilic character, less branched and smaller molecular size of QSP resulted in longer T_2 times ($p < 0.05$). Oil addition to these gum solutions decreased the T_2 of both samples as expected but the longer T_2 trend for QSP including samples remained. QSP also interacted with oil droplets to some extent but XG chains continued to interact extensively with the water phase. In contrast to these results, longer T_2 trend of QSP containing gum solutions was reversed in the presence of WPI. WPI decreased the T_2 values of the gum solutions but this time XG-WPI-water samples had longer T_2 times ($p < 0.05$). Electrostatic interactions between the positive patches of WPI and anionic XG side chains provided a reduction in the polysaccharide – water interactions. Consequently, these samples had longer T_2 times ($p < 0.05$). When oil was incorporated into the gum-WPI-water systems, the general T_2 trend for QSP containing samples was observed again. Surface active properties of both WPI and QSP enabled them to interact on the interface but only the hydrophilic fraction of WPI interacted with water in the aqueous phase. On the other hand, steric incompatibility between the WPI and XG molecules promoted a higher amount of protein adsorption on the oil droplets [47]. Energy exchange rate at the emulsion interface increased and XG restricted the mobility of the water molecules in the continuous phase. Thus, inevitably, XG-WPI-oil-water emulsions attained shorter T_2 ($p < 0.05$) values.

Lastly, AL was added to the emulsion formulations. AL predominated the transverse relaxation process of water in the gum solutions since QSP-AL-Water and XG-AL-Water solutions had similar T_2 times. XG and AL are both classified as non-adsorbing polysaccharides [34]. Therefore, XG and AL together, interacted strongly with the water in the aqueous phase. In addition, similar T_2 times of QSP-AL-Water system indicated the dominant hydrophilic behavior of AL. As a supportive observation for that claim, AL decreased the T_2 of gum solutions more effectively compared to WPI ($p < 0.05$). Presence of oil in the same AL containing systems resulted in shorter T_2 times for both emulsions but QSP-AL-Oil-Water samples had longer T_2 times than their XG correspondents ($p < 0.05$). This result was also related to the amphiphilic character of QSP.

Finally, QSP-AL-WPI-Oil-Water and XG-AL-WPI-Oil-Water emulsions, *(the ones used for Ca^{2+} induced gels)*, were prepared. These QSP and XG emulsions were found to have similar T_2 values probably due to the presence of all emulsifiers at the same time within the emulsions. Conformational arrangements of globular proteins like WPI constituents and rigid anionic polysaccharides played a crucial role in their interactions since all charged groups could not contact efficiently due to the conformational limitations [48]. But, AL had negative charge over a wide pH range and this enabled electrostatic interactions between

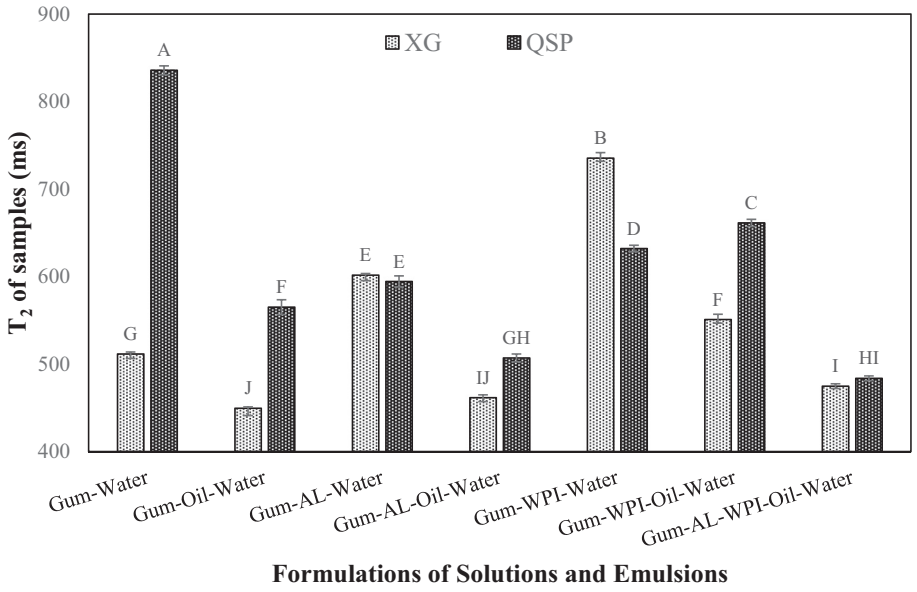

Fig. 6. Transverse relaxation times of all emulsion formulations ($p < 0.05$). Gums represent either XG or QSP. Error bars are represented as standard errors.

WPI and AL leading to stable emulsions [49]. In this case, the dominant factor for emulsion stabilization was the viscosity of the continuous phase. The lower mean particle size of XG emulsions agreed with this finding (Fig. 4). Lower particle size values are generally associated with more stable systems [49].

3.3.1.2. Hydrogels. T_2 results of the hydrogels showed a monoexponential behavior and did not yield a multi relaxation behavior. Gels obtained by Ca^{2+} induced gelation of gum-AL-WPI-Oil-Water emulsions showed that XG gels had the longest T_2 times while QSP and Control emulsions achieved similar but shorter T_2 values ($p < 0.05$) (Fig. 7). During gelling, QSP, XG and Control emulsions were subjected to 0.25 M $CaCl_2$ solution with an ionic strength of 0.75. Interactions between the WPI and the added polysaccharides in the continuous phase was modified by the ions present in the emulsion. Association of the WPI molecules highly depended on the ion concentration in the system [50]. Anionic side chains of XG interacted extensively with Ca^{2+} ions during gelling and a stiff conformation of XG was established. Therefore, XG gels created distinct water pools within its structure and immobilized water in these compartments resulted in longer T_2 times [13]. Presence of QSP could not produce such compartments due to its lower association with Ca^{+2} with respect to XG. Extracts of quince seeds contain cellulose, hemicellulose, lignin and water soluble polysaccharides such as glucan, galacto-glucan and arabino-xylan fractions [5,7]. QSP also possesses a high dietary fiber content and gum constituents. These fibers and gums have a good water-binding capacity leading to higher viscosities in the QSP containing solutions [40,51]. QSP was reported to have both thickening and amphiphilic properties [6,51]. The amphiphilic characteristics of QSP originated from its protein fraction and hydrophobic methylene groups [5]. These fractions enabled QSP molecules to adsorb onto the hydrophobic oil droplet surfaces and form a strong interfacial layer [51]. On the other hand, high molecular weight polysaccharides of QSP provided emulsion stabilization and a gelation behavior in the solutions [52]. All these properties of QSP resulted in a shorter T_2 values for its gels ($p < 0.05$). Presence of WPI and AL contributed to the gelation of Control samples in the absence of QSP or XG. Divalent cations interacted with guluronate blocks of AL to form an egg-box model gel like structures [9]. By this way, junction zones between the adjacent chains were created giving a three-dimensional weak gel network [53]. AL molecules located in the aqueous phase of the emulsions could interact with surfactants adsorbed on the oil droplets through electrostatic repulsion and steric interactions [54]. Depending of the pH of the solution, globular proteins were reported to form soluble or insoluble complexes with AL molecules in the aqueous phase [55]. Therefore, *Control* emulsions were also able to gel under the same conditions with XG and QSP emulsions and they had gelling characteristics closer to QSP gels.

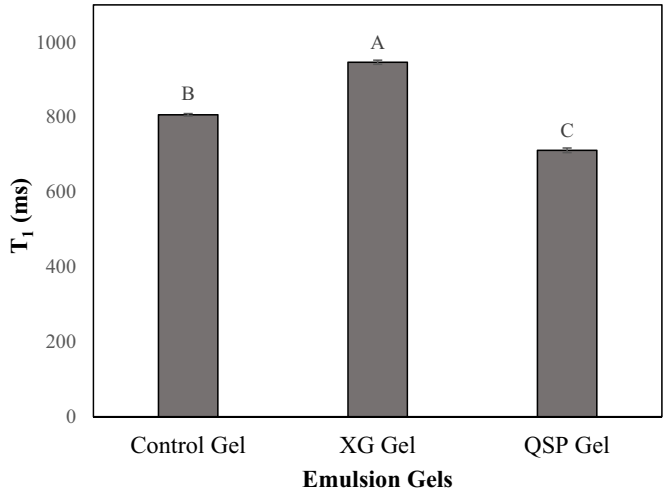

Fig. 7. Transverse relaxation (T_2) times of the gels ($p < 0.05$). Control, XG and QSP gels represent the formulations; AL-WPI-Oil-Water, XG-AL-WPI-Oil-Water, QSP-AL-WPI-Oil-Water, respectively. Error bars are represented as standard errors.

3.3.2. Transverse relaxation spectrum analysis of emulsions

For emulsions, as stated before a *multiexponential relaxation time distribution* analysis was also performed. Table 3 summarizes the relaxation spectrum of oil containing emulsions. These samples had two distinct proton populations with their respective peak times and areas [46]. First peaks having shorter peak times and lower areas were attributed to the contribution of dispersed oil phase to the relaxation since oil had much shorter T_2 than water [56]. QSP-Oil-Water and QSP-WPI-Oil-Water formulations had longer T_2 in peak 1 than their correspondent XG formulations indicating the emulsifier effect of QSP ($p < 0.05$). A longer peak 1 time showed that water in the continuous aqueous phase was able to participate in the interactions on the interface resulted in longer T_2 values for this peak. XG was known as a non-adsorbing

Table 3
Transverse relaxation spectrum analysis of all emulsion formulations. Different letters in each column mean emulsion type differed significantly ($p < 0.05$). Errors are represented as standard deviations.

Emulsion	T_{21} (ms)	RA_1 (%)	T_{22} (ms)	RA_2 (%)
QSP-oil-water	81 ± 4^{a}	14 ± 1^{a}	627 ± 23^{b}	86 ± 1^{e}
QSP-WPI-oil-water	66 ± 4^{b}	13 ± 1^{ab}	693 ± 40^{a}	87 ± 1^{de}
QSP-AL-oil-water	56 ± 2^{c}	10 ± 1^{cd}	550 ± 17^{c}	90 ± 1^{bc}
QSP-AL-WPI-oil-water	37 ± 2^{d}	6 ± 1^{e}	490 ± 1^{d}	94 ± 1^{a}
XG-oil-water	62 ± 2^{bc}	9 ± 1^{d}	460 ± 1^{d}	91 ± 1^{b}
XG-WPI-oil-water	54 ± 3^{c}	12 ± 1^{abc}	600 ± 1^{b}	88 ± 1^{cde}
XG-AL-oil-water	57 ± 1^{c}	12 ± 1^{bc}	490 ± 1^{d}	89 ± 1^{cd}
XG-AL-WPI-oil-water	32 ± 3^{d}	9 ± 1^{d}	490 ± 1^{d}	91 ± 1^{b}

polymer thus it was not expected that the T_2 of the proton pool that was attributed to the oil would attract water and had a longer relaxation time in the solution of a non-adsorbing polymer. Therefore, XG-Oil-Water and XG-WPI-Oil-Water samples had shorter peak 1 times ($p < 0.05$). Moreover, addition of AL to Gum-Oil-Water and Gum-WPI-Oil-Water systems resulted in a shorter peak 1 T_2 ($p < 0.05$) compared to non-AL systems and similar peak times were observed for QSP and XG systems. Hydrophilic character of AL dominated the continuous phase of the emulsions and abundance of interactions between the water phase and oil phase was replaced by AL – water interactions. It was hypotheiszed that QSP solutions are more susceptible to WPI and AL addition in terms of shorter peak 1 times which was mainly due to surface active property of QSP rather than viscosity increasing effect in the bulk phase. When AL and WPI were present in the emulsions at the same time, continuous phase viscosity properties determined the peak 1-time values.

Areas of peak 1 obtained from the relaxation spectrum (Table 3) suggested that QSP and WPI were surface active polymers which was in agreement with the literature findings [5,57]. WPI molecules were reported to act as emulsifiers and during homogenization they migrated to oil-water interfaces. Hydrophobic adsorption sites of WPI anchor on the oil droplet surface. After covering the droplet surface, WPI molecules start to form a viscoelastic film contributing to steric stabilization of the system [49]. WPI adsorbs on the droplet surfaces layer by layer and the first layer behaves as the substrate for further adsorption of WPI molecules [58]. Moreover, Sun et al. (2009) reported that WPI was effective on determining the surface charge of oil droplets [59]. On the other hand, Ritzoulis et al. (2014) stated that quince seed extracts that they analyzed contained substantial amounts of protein ranging from 10% to 25%. Presence of protein in the quince seeds played a crucial role on the adsorption of QSP molecules on the droplets [5]. In our case, this protein fraction of the QSP could have caused electrostatic repulsion at the interface and stabilized the systems [5,60]. Peak 1 area values as shown in Table 3 were compatible with these findings. Firstly, QSP-Oil-Water system had higher peak 1 area than XG-Oil-Water system showing the surface activity of QSP ($p < 0.05$). A higher area for the first peak suggested the presence of a higher rate of interaction in this proton population. When WPI was added to the Gum-Oil-Water emulsions, relative peak areas of QSP and XG added samples attained similar values ($p < 0.05$). This indicated that WPI was more dominant than QSP molecules in terms of providing surface activity on the interphase. AL addition also revealed statistically the same peak 1 area ($p > 0.05$). Predominant effect of WPI was also observed in Gum-AL-WPI-Oil-Water combinations since XG containing emulsions had higher peak 1 area compared to the relative peak area of QSP emulsions ($p < 0.05$). WPI – AL biopolymeric interface acted as an anchor between the oil droplet surface and the aqueous continuous phase [61]. This result was quite opposite to the area values of Gum-Oil-Water formulations. WPI with its bigger molecular size and amphiphilic patches predominated the interactions on the oil droplets independent from the gum type that was added to the formulation.

Peak 2 was associated with the interactions mainly taking place in the aqueous phase of the emulsions and revealed considerably longer T_2 than peak 1 (Table 3) [62]. Most of the emulsion combinations including QSP attained longer T_2 times than XG containing formulations for the second peak ($p < 0.05$). Only Gum-AL-WPI-Oil-Water combinations attained statistically the same peak times ($p > 0.05$). Shorter peak times of XG blended samples proved the enhanced interaction of XG molecules with the surrounding water molecules in the aqueous phase. Simultaneous presence of WPI and AL in the emulsions predominated the physicochemical properties in the continuous phase and similar T_2's at peak 2 were observed. Peak 2 areas were substantially higher than peak 1 areas indicating the importance of the continuous phase's contribution on the stability of the emulsions ($p < 0.05$) [6]. WPI and AL containing emulsions generally promoted more interactions within the system and resulted in higher relative areas ($p < 0.05$). XG-Oil-Water emulsions had a higher relative peak area compared to QSP-Oil-Water emulsions as expected ($p < 0.05$). However, peak 2 area of QSP-AL-WPI-Oil-Water formulations attained higher area values with respect to their correspondent XG emulsions ($p < 0.05$). This reverse correlation between the peak 2 areas for the aforementioned formulations indicated that WPI and AL affected the continuous phase properties substantially. Although XG was the predominant component for the regulating the rheological properties of the aqueous phase, interactions in this phase also depended strongly on WPI and AL actions. In general, the proton relaxation compartment described by peak 2 simulated the overall monoexponential T_2 results of the emulsions. Similar overall T_2 for QSP and XG emulsions for the final formulations supported these findings.

3.3.3. Longitudinal relaxation results of gels

For hydrogels, T_1 relaxation times were also measured and the data fitted well with mono exponential as in the case of T_2. Longitudinal or spin – lattice relaxation time represents the energy exchange rate of ^1H protons with the surrounding lattice [27]. Fig. 8 shows the T_1 times of Ca^{+2} induced emulsion gels having gum (QSP or XG), AL, WPI, oil and water. XG gels had the longest T_1 which was consistent with its T_2 results ($p < 0.05$). Local water populations not interacting with the surrounding polymer lattice relaxed slowly in XG gels. In addition, XG molecules with no or negligible surface activity did not commit energy exchange reactions with the oil droplets. These reactions were only carried out by WPI molecules which was not sufficient to attain high energy exchange rates that would reduce the T_1 of XG gels. QSP gels had the shortest T_1 times and the main reason was the interfacial activity of QSP molecules on the oil droplets ($p < 0.05$). QSP molecules adsorbed on the oil-water interface could have experienced intense proton

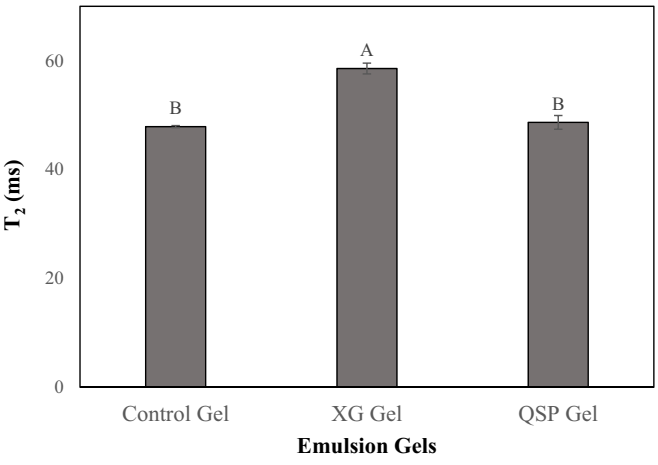

Fig. 8. Longitudinal relaxation times (T_1) of the gels ($p < 0.05$). Control, XG and QSP gels represent the formulations; AL-WPI-Oil-Water, XG-AL-WPI-Oil-Water, QSP-AL-WPI-Oil-Water, respectively. Error bars are represented as standard errors.

Table 4
T_2 results obtained from the MR images. Control, XG and QSP gels represent the formulations; AL-WPI-Oil-Water, XG-AL-WPI-Oil-Water, QSP-AL-WPI-Oil-Water, respectively. Different letters in each column mean gel type differed significantly ($p < 0.05$). Errors are represented as standard deviations. (RA means 'relative area' and denotes the contribution of that peak to the signal).

Gel	T_{21} (ms)	T_{22} (ms)	RA_1 (%)	RA_2 (%)
Control	52.28 ± 0.99^{ab}	108.93 ± 2.27^{b}	60.90 ± 1.31^{c}	39.10 ± 1.31^{c}
QSP	50.38 ± 0.40^{b}	127.57 ± 1.62^{a}	81.50 ± 0.44^{a}	18.50 ± 0.44^{a}
XG	53.59 ± 0.83^{a}	103.53 ± 2.57^{b}	64.43 ± 2.85^{b}	35.57 ± 2.85^{b}

exchange rate with the surrounding molecules thus longitudinal relaxation process was faster for these samples [63]. Control gels had moderate T_1 times which was consistent with the emulsification capabilities of the added XG and QSP polymers.

3.4. MRI results for hydrogels

T_2 results obtained from MR Images were different than the results found in the low field system. Although the signal to noise (SNR) values were quite high in the low field systems, the field being not homogenous enough and the fast exchange rate at low field might have prevented the detection of two compartments thus one component was observed, and results were interpreted accordingly. However, MR images showed the presence of two compartments in emulsion gels. First component's T_2 times changed between 50 and 55 ms whereas for the second component T_2 values were in the range of 100–130 ms. Results for different hydrogels and the contribution of each peak to the overall signal is given in Table 4.

Since it is known that oil had a relaxation time that could change between 90 and 120 ms, second compartment was associated with protons coming from the oil present in the gels whereas first component denoted the protons that were strongly interacting with the polymer matrix. For the first component XG and QSP hydrogels were significantly different from each other ($p < 0.05$) indicating that polymer water interaction was stronger in the QSP gels. But since quince had also emulsifying ability, contribution of oil could have also decreased the relaxation times. The difference was also obvious in the second component as the second component had the longest T_2 which was indicative of the good emulsifying ability of QSP. as QSP helped to disperse oil much better in the continuous phase and also had exchanging proton contributions from the water phase. The high contribution of the first component was also a good indication showing that QSP gels were more homogenous and emulsified much better as the contribution was significantly higher compared to control and XG samples. This was also consistent with the fact that QSP hydrogels had the shortest T_2 for the first component indicating a strong gel network with the oil phase.

In addition to relaxation times, T_2 maps were also evaluated. As seen in Fig. 3 and previously in gel photos (Fig. 1), there was oil accumulation in the center. Accumulation of the oil phase in the center indicated the instability. There is a significant signal intensity difference between the center and the edges. This was quantified by calculating the standard deviation on the T_2 maps as seen in the Fig. 3. For control samples standard deviation was quite high and when ANOVA was conducted between XG and QSP samples it was seen that QSP hydrogels significantly had lower deviations than the XG hydrogels.

3.5. SEM images

Control gels had a smooth structure in the absence of QSP or XG, as shown in the SEM image (Fig. 9A). These gels possessed large clumps on the relatively plain background. Fig. 9B shows the QSP gel image having random sized droplet structures on the surface. QSP as an adsorbing polymer probably coated the droplets to some extent with WPI contribution. The nonhomogeneous size distribution of the clumpy structures

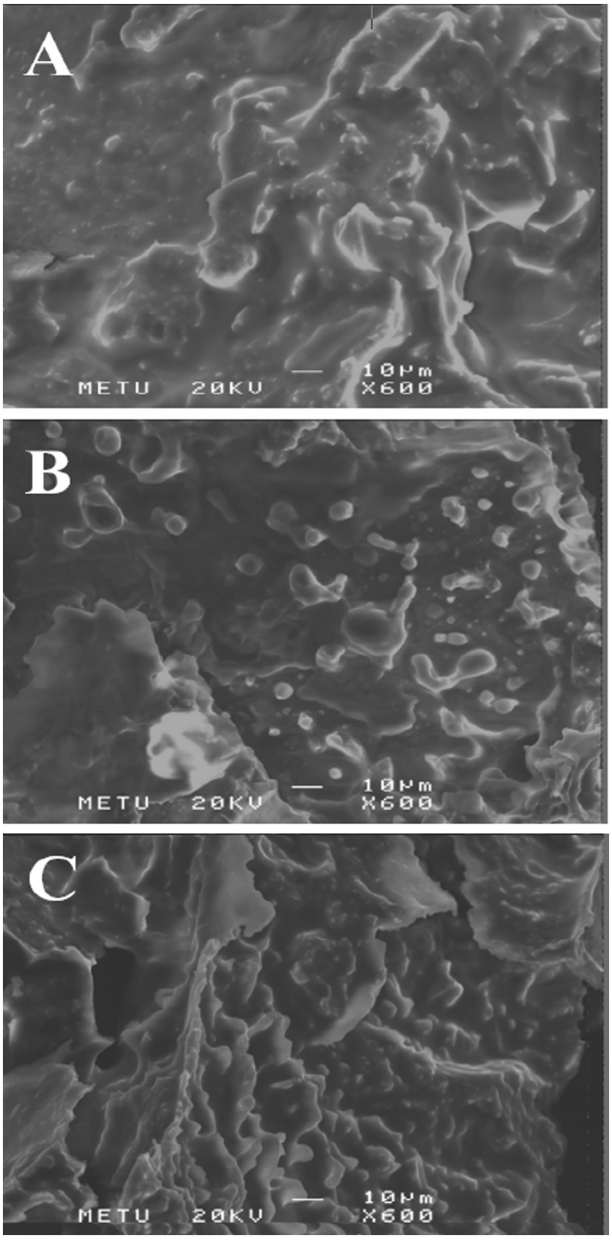

Fig. 9. SEM images of the gels: (a) Control, (b) QSP, (c) XG. Control, QSP and XG gels represent the formulations; AL-WPI-Oil-Water, QSP-AL-WPI-Oil-Water, XG-AL-WPI-Oil-Water, respectively.

was due to the insufficient continuous phase viscosity of the QSP emulsions and during gelling this caused a random distribution of the coated droplets. XG gel (Fig. 9C) exerted a filamentous and fragmented structure with denser and smaller clumps [64]. These structures could be attributed to the branched network of XG and the resulting intense interactions with the added Ca^{+2} ions during gelation [40]. The abundance and complexity of anionic side chains led to a more distorted texture for XG gels with respect to Control and QSP gels.

4. Conclusion

QSP and XG blended emulsion formulations were characterized mainly by NMR relaxometry transverse and longitudinal relaxation parameters. A detailed relaxation spectrum analysis of biexponential samples was also conducted. NMR results were discussed together with mean particle size, rheology and SEM image analyses. Consequently, XG based emulsions produced lower particle size systems with respect

to QSP including samples, in the presence of WPI and AL as additional polymers. It was demonstrated that the interactions of non-adsorbing XG and adsorbing QSP molecules within the o/w emulsions could be monitored by T_2 measurements. The longest T_1 and T_2 results of XG emulsion gels agreed with the lower particle size distribution of respective XG emulsions ($p < 0.05$). T_1 and T_2 decreasing effect of oil lumps were compensated by smaller and more homogenous oil droplet distribution within the XG gels. However, MR images provided more info on the relaxation time of hydrogels. Relaxation spectrum analysis denoted the presence of two compartments. High contribution and short relaxation time of the first peak confirmed the emulsification ability of QSP in hydrogels. Moreover, T_2 maps revealed that hydrocolloids definitely improved the stability of the gels as observed on the deviations obtained from T_2 maps. In overall, it was shown that QSP would be a good alternative to be used in emulsions and hydrogel systems.

Funding

A part of the funding for this study came from Dr. Oztop's award of Science Academy Young Scientist Awards Program (BAGEP).

Declaration of competing of interest

All authors declare no conflict of interest.
Publication has been approved by all individual participants.

Acknowledgment

The authors would like to thank UMRAM (National Magnetic Resonance Center at Bilkent University, Ankara, Turkey) as MRI experiments were performed by using the clinical scanner there.

COST Action CA 15209 European Network on Relaxometry is also acknowledged as some of the findings are discussed in the action's network meetings and suggestions were taken into consideration in the final text.

Author statement

- The PI of the project was Dr. Oztop and he coordinated the project and finalized the manuscript with Dr. Sahin.
- The topic was assigned as the MSc thesis of Mrs. İrem Alacik Develioglu
- Baris Ozel created the 1st draft of the manuscript and conducted all the required analysis for the manuscript.

Appendix A. Supplementary data

Supplementary data to this article can be found online at https://doi.org/10.1016/j.ijbiomac.2020.08.087.

References

[1] X. Huang, Y. Kakuda, W. Cui, Hydrocolloids in emulsions: particle size distribution and interfacial activity, Food Hydrocoll. 15 (2001) 533–542, https://doi.org/10.1016/S0268-005X(01)00091-1.
[2] E. Dickinson, Hydrocolloids as emulsifiers and emulsion stabilizers, Food Hydrocoll. 23 (2009) 1473–1482, https://doi.org/10.1016/j.foodhyd.2008.08.005.
[3] C. Sun, S. Gunasekaran, M.P. Richards, Effect of xanthan gum on physicochemical properties of whey protein isolate stabilized oil-in-water emulsions, Food Hydrocoll. 21 (2007) 555–564, https://doi.org/10.1016/j.foodhyd.2006.06.003.
[4] Y. Hemar, M. Tamehana, P.A. Munro, H. Singh, Influence of xanthan gum on the formation and stability of sodium caseinate oil-in-water emulsions, Food Hydrocoll. 15 (2001) 513–519, https://doi.org/10.1016/S0268-005X(01)00075-3.
[5] C. Ritzoulis, E. Marini, A. Aslanidou, N. Georgiadis, P.D. Karayannakidis, C. Koukiotis, A. Filotheou, S. Lousinian, E. Tzimpilis, Hydrocolloids from quince seed: extraction, characterization, and study of their emulsifying/stabilizing capacity, Food Hydrocoll. 42 (2014) 178–186, https://doi.org/10.1016/j.foodhyd.2014.03.031.
[6] E. Kirtil, M.H. Oztop, Characterization of emulsion stabilization properties of quince seed extract as a new source of hydrocolloid, Food Res. Int. 85 (2016) 84–94, https://doi.org/10.1016/j.foodres.2016.04.019.
[7] T.J. Hakala, V. Saikko, S. Arola, T. Ahlroos, A. Helle, P. Kuosmanen, K. Holmberg, M.B. Linder, P. Laaksonen, Structural characterization and tribological evaluation of quince seed mucilage, Tribol. Int. 77 (2014) 24–31, https://doi.org/10.1016/j.triboint.2014.04.018.
[8] E. Dickinson, Hydrocolloids at interfaces and the influence on the properties of dispersed systems, Food Hydrocoll. 17 (2003) 25–39.
[9] K.Y. Lee, D.J. Mooney, Alginate: properties and biomedical applications, Prog. Polym. Sci. 37 (2012) 106–126, https://doi.org/10.1016/j.progpolymsci.2011.06.003.
[10] M. George, T.E. Abraham, Polyionic hydrocolloids for the intestinal delivery of protein drugs: alginate and chitosan - a review, J. Control. Release 114 (2006) 1–14, https://doi.org/10.1016/j.jconrel.2006.04.017.
[11] G. Liling, Z. Di, X. Jiachao, G. Xin, F. Xiaoting, Z. Qing, Effects of ionic crosslinking on physical and mechanical properties of alginate mulching films, Carbohydr. Polym. 136 (2016) 259–265, https://doi.org/10.1016/j.carbpol.2015.09.034.
[12] E. Kirtil, M.H. Oztop, H nuclear magnetic resonance Relaxometry and magnetic resonance imaging and applications in food science and processing, Food Eng. Rev. (2016) 1–22, https://doi.org/10.1007/s12393-015-9118-y.
[13] B. Ozel, S.S. Uguz, M. Kilercioglu, L. Grunin, M.H. Oztop, Effect of different polysaccharides on swelling of composite whey protein hydrogels: a low field (LF) NMR relaxometry study, J. Food Process Eng. 40 (2017) 1–9, https://doi.org/10.1111/jfpe.12465.
[14] B. Ozel, D. Dag, M. Kilercioglu, S.G. Sumnu, M.H. Oztop, NMR relaxometry as a tool to understand the effect of microwave heating on starch-water interactions and gelatinization behavior, LWT - Food Sci. Technol. 83 (2017) 10–17, https://doi.org/10.1016/j.lwt.2017.04.077.
[15] B. Ozel, O. Aydin, L. Grunin, M.H. Oztop, Physico-chemical changes of composite whey protein hydrogels in simulated gastric fluid conditions, J. Agric. Food Chem. 66 (2018) 9542–9555, https://doi.org/10.1021/acs.jafc.8b02829.
[16] S. Sevdin, B. Ozel, U. Yucel, M.H. Oztop, H. Alpas, High hydrostatic pressure induced changes on palm stearin emulsions, J. Food Eng. 229 (2018) 65–71, https://doi.org/10.1016/j.jfoodeng.2017.10.007.
[17] E. Kirtil, D. Dag, S. Guner, K. Unal, M.H. Oztop, Dynamics of unloaded and green tea extract loaded lecithin based liposomal dispersions investigated by nuclear magnetic resonance T2 relaxation, Food Res. Int. (2017)https://doi.org/10.1016/j.foodres.2017.06.064.
[18] E. Kirtil, M.H. Oztop, Characterization of emulsion stabilization properties of quince seed extract as a new source of hydrocolloid, Food Res. Int. 85 (2016) 84–94, https://doi.org/10.1016/j.foodres.2016.04.019.
[19] P. Pocan, E. Ilhan, M.H. Oztop, Effect of d-psicose substitution on gelatin based soft candies: a TD-NMR study, Magn. Reson. Chem. 57 (2019) 661–673, https://doi.org/10.1002/mrc.4847.
[20] E. Ilhan, P. Pocan, M. Ogawa, M.H. Oztop, Role of 'D-allulose' in a starch based composite gel matrix, Carbohydr. Polym. 228 (2020), 115373https://doi.org/10.1016/j.carbpol.2019.115373.
[21] R. de O.R. Ribeiro, E.T. Mársico, C. da S. Carneiro, M.L.G. Monteiro, C.C. Júnior, E.F.O. de Jesus, Detection of honey adulteration of high fructose corn syrup by low field nuclear magnetic resonance (LF 1H NMR), J. Food Eng. 135 (2014) 39–43, https://doi.org/10.1016/j.jfoodeng.2014.03.009.
[22] S. Ok, Detection of olive oil adulteration by low-field NMR relaxometry and UV-Vis spectroscopy upon mixing olive oil with various edible oils, Grasas Aceites 68 (2017) 173, https://doi.org/10.3989/gya.0678161.
[23] P.M. Santos, E.R. Pereira-filho, L.A. Colnago, Detection and quanti fi cation of milk adulteration using time domain nuclear magnetic resonance (TD-NMR), Microchem. J. 124 (2016) 15–19, https://doi.org/10.1016/j.microc.2015.07.013.
[24] M. Ladd-Parada, M.J. Povey, J. Vieira, M.E. Ries, Fast field cycling NMR relaxometry studies of molten and cooled cocoa butter, Mol. Phys. (2018)https://doi.org/10.1080/00268976.2018.1508784.
[25] M. Adam-Berret, C. Rondeau-Mouro, A. Riaublanc, F. Mariette, Study of triacylglycerol polymorphs by nuclear magnetic resonance: effects of temperature and chain length on relaxation parameters, Magn. Reson. Chem. 46 (2008) 550–557, https://doi.org/10.1002/mrc.2213.
[26] P.D. Williams, M.H. Oztop, M.J. McCarthy, K.L. McCarthy, Y.M. Lo, Characterization of water distribution in xanthan-Curdlan hydrogel complex using magnetic resonance imaging, nuclear magnetic resonance relaxometry, rheology, and scanning electron microscopy, J. Food Sci. 76 (2011) E472–E478, https://doi.org/10.1111/j.1750-3841.2011.02227.x.
[27] R.H. Hashemi, W.G. Bradley, C.J. Lisanti, MRI: The Basics, Lippincott Williams & Wilkins, 2010.
[28] M.H. Oztop, M. Rosenberg, Y. Rosenberg, K.L. McCarthy, M.J. McCarthy, Magnetic resonance imaging (MRI) and relaxation spectrum analysis as methods to investigate swelling in whey protein gels, J. Food Sci. 75 (2010) E508–E515, https://doi.org/10.1111/j.1750-3841.2010.01788.x.
[29] F. Kong, M.H. Oztop, R. Paul Singh, M.J. McCarthy, Effect of boiling, roasting and frying on disintegration of peanuts in simulated gastric environment, LWT - Food Sci. Technol. 50 (2013) 32–38.
[30] F. Kong, M.H. Oztop, R.P. Singh, M.J. Mccarthy, Physical changes in white and brown rice during simulated gastric digestion, J. Food Sci. 76 (2011).
[31] A. Altan, D.M. Lavenson, M.J. Mccarthy, K.L. Mccarthy, Oil migration in chocolate and almond product confectionery systems, J. Food Sci. 76 (2011)https://doi.org/10.1111/j.1750-3841.2011.02233.x.
[32] S. Cikrikci, M.H. Oztop, Mathematical modeling and use of magnetic resonance imaging (MRI) for oil migration in chocolate confectionery systems, Food Eng. Rev. (2016)https://doi.org/10.1007/s12393-016-9152-4.
[33] T. Defraeye, V. Lehmann, D. Gross, C. Holat, E. Herremans, P. Verboven, B.E. Verlinden, B.M. Nicolai, Application of MRI for tissue characterisation of "Braeburn"

apple, Postharvest Biol. Technol. 75 (2013) 96–105, https://doi.org/10.1016/j.postharvbio.2012.08.009.
[34] E. Bouyer, G. Mekhloufi, V. Rosilio, J.L. Grossiord, F. Agnely, Proteins, polysaccharides, and their complexes used as stabilizers for emulsions: alternatives to synthetic surfactants in the pharmaceutical field? Int. J. Pharm. 436 (2012) 359–378, https://doi.org/10.1016/j.ijpharm.2012.06.052.
[35] S. Wichchukit, M.H. Oztop, M.J. McCarthy, K.L. McCarthy, Whey protein/alginate beads as carriers of a bioactive component, Food Hydrocoll. 33 (2013) 66–73, https://doi.org/10.1016/j.foodhyd.2013.02.013.
[36] S. Cikrikci, B. Mert, M.H. Oztop, Development of pH sensitive alginate/gum Tragacanth based hydrogels for Oral insulin delivery, J. Agric. Food Chem. 66 (2018) 11784–11796, https://doi.org/10.1021/acs.jafc.8b02525.
[37] G. Lozano-Vazquez, C. Lobato-Calleros, H. Escalona-Buendia, G. Chavez, J. Alvarez-Ramirez, E.J. Vernon-Carter, Effect of the weight ratio of alginate-modified tapioca starch on the physicochemical properties and release kinetics of chlorogenic acid containing beads, Food Hydrocoll. 48 (2015) 301–311, https://doi.org/10.1016/j.foodhyd.2015.02.032.
[38] B. Ozel, S.S. Uguz, M. Kilercioglu, L. Grunin, M.H. Oztop, Effect of different polysaccharides on swelling of composite whey protein hydrogels: a low field (LF) NMR relaxometry study, J. Food Process Eng. (2016) 1–9, https://doi.org/10.1111/jfpe.12465.
[39] C.E. Brunchi, M. Avadanei, M. Bercea, S. Morariu, Chain conformation of xanthan in solution as influenced by temperature and salt addition, J. Mol. Liq. 287 (2019), 111008https://doi.org/10.1016/j.molliq.2019.111008.
[40] L. Wang, H.M. Liu, A.J. Xie, X. De Wang, C.Y. Zhu, G.Y. Qin, Chinese quince (Chaenomeles sinensis) seed gum: structural characterization, Food Hydrocoll. 75 (2018) 237–245, https://doi.org/10.1016/j.foodhyd.2017.08.001.
[41] E. Vega, E. Vásquez, J. Diaz, M. Masuelli, Influence of the ionic strength in the intrinsic viscosity of xanthan gum. An experimental review, J. Polym. Biopolym. Phys. Chem. 3 (2015) 12–18, https://doi.org/10.12691/jpbpc-3-1-3.
[42] S. Hemmatzadeh, M. Hojjatoleslamy, O. Eivazzadeh, Hemmatzadeh effect of ph and calcium salt on rehological properties of XG carboxymethyl cellulose blends, Annu. Trans. Nord. Rheol. Soc (2011) 19.
[43] C.M. Bryant, D.J. McClements, Influence of xanthan gum on physical characteristics of heat-denatured whey protein solutions and gels, Food Hydrocoll. 14 (2000) 383–390, https://doi.org/10.1016/S0268-005X(00)00018-7.
[44] C. Sanchez, C. Schmitt, V.G. Babak, J. Hardy, Rheology of whey protein isolate-xanthan mixed solutions and gels. Effect of pH and xanthan concentration, Nahrung – Food 41 (1997) 336–343, https://doi.org/10.1002/food.19970410604.
[45] B. Abbastabar, M.H. Azizi, A. Adnani, S. Abbasi, Determining and modeling rheological characteristics of quince seed gum, Food Hydrocoll. 43 (2015) 259–264, https://doi.org/10.1016/j.foodhyd.2014.05.026.
[46] F. Mariette, Investigations of food colloids by NMR and MRI, Curr. Opin. Colloid Interface Sci. 14 (2009) 203–211, https://doi.org/10.1016/j.cocis.2008.10.006.
[47] E.M. Papalamprou, E.A. Makri, V.D. Kiosseoglou, G.I. Doxastakis, Effect of medium molecular weight xanthan gum in rheology and stability of oil-in-water emulsion stabilized with legume proteins, J. Sci. Food Agric. 85 (2005) 1967–1973, https://doi.org/10.1002/jsfa.2159.
[48] V.B. Tolstoguzov, Some thermodynamic considerations in food formulation, Food Hydrocoll. 17 (1) (2003).
[49] K.M. Albano, Â.L.F. Cavallieri, V.R. Nicoletti, Electrostatic interaction between proteins and polysaccharides: physicochemical aspects and applications in emulsion stabilization, Food Rev. Int. 35 (2019) 54–89, https://doi.org/10.1080/87559129.2018.1467442.
[50] V.Y. Grinberg, V.B. Tolstoguzov, Thermodynamic incompatibility of proteins and polysaccharides in solutions, Food Hydrocoll. 11 (1997) 145–158, https://doi.org/10.1016/S0268-005X(97)80022-7.
[51] A. Kurt, I. Atalar, Food hydrocolloids effects of quince seed on the rheological, structural and sensory characteristics of ice cream, Food Hydrocoll. 82 (2018) 186–195, https://doi.org/10.1016/j.foodhyd.2018.04.011.
[52] M. Jouki, S.A. Mortazavi, F.T. Yazdi, A. Koocheki, Optimization of extraction, antioxidant activity and functional properties of quince seed mucilage by RSM, Int. J. Biol. Macromol. 66 (2014) 113–124, https://doi.org/10.1016/j.ijbiomac.2014.02.026.
[53] S.K. Bajpai, R. Tankhiwale, Investigation of water uptake behavior and stability of calcium alginate/chitosan bi-polymeric beads: Part-1, React. Funct. Polym. 66 (2006) 645–658, https://doi.org/10.1016/j.reactfunctpolym.2005.10.017.
[54] M. Artiga-Artigas, A. Acevedo-Fani, O. Martín-Belloso, Effect of sodium alginate incorporation procedure on the physicochemical properties of nanoemulsions, Food Hydrocoll. 70 (2017) 191–200, https://doi.org/10.1016/j.foodhyd.2017.04.006.
[55] M.G. Sosa-Herrera, I.E. Lozano-Esquivel, Y.R. Ponce de León-Ramírez, L.P. Martínez-Padilla, Effect of added calcium chloride on the physicochemical and rheological properties of aqueous mixtures of sodium caseinate/sodium alginate and respective oil-in-water emulsions, Food Hydrocoll. 29 (2012) 175–184, https://doi.org/10.1016/j.foodhyd.2012.02.017.
[56] N. Marigheto, L. Venturi, D. Hibberd, K.M. Wright, G. Ferrante, B.P. Hills, Methods for peak assignment in low-resolution multidimensional NMR cross-correlation relaxometry, J. Magn. Reson. 187 (2007) 327–342, https://doi.org/10.1016/j.jmr.2007.04.016.
[57] E. Dickinson, Flocculation of protein-stabilized oil-in-water emulsions, Colloids Surfaces B Biointerfaces 81 (2010) 130–140, https://doi.org/10.1016/j.colsurfb.2010.06.033.
[58] S. Tcholakova, N.D. Denkov, I.B. Ivanov, B. Campbell, Coalescence in β-lactoglobulin-stabilized emulsions: effects of protein adsorption and drop size, Langmuir 18 (2002) 8960–8971, https://doi.org/10.1021/la0258188.
[59] C. Sun, S. Gunasekaran, Effects of protein concentration and oil-phase volume fraction on the stability and rheology of menhaden oil-in-water emulsions stabilized by whey protein isolate with xanthan gum, Food Hydrocoll. 23 (2009) 165–174, https://doi.org/10.1016/j.foodhyd.2007.12.006.
[60] S. Tcholakova, N.D. Denkov, D. Sidzhakova, I.B. Ivanov, B. Campbell, Effects of electrolyte concentration and pH on the coalescence stability of β-lactoglobulin emulsions: experiment and interpretation, Langmuir 21 (2005) 4842–4855, https://doi.org/10.1021/la046891w.
[61] A.M. Leon, W.T. Medina, D.J. Park, J.M. Aguilera, Properties of microparticles from a whey protein isolate/alginate emulsion gel, Food Sci. Technol. Int. 24 (2018) 414–423, https://doi.org/10.1177/1082013218762210.
[62] L. Vermeir, M. Balcaen, P. Sabatino, K. Dewettinck, P. Van der Meeren, Influence of molecular exchange on the enclosed water volume fraction of W/O/W double emulsions as determined by low-resolution NMR diffusometry and T2-relaxometry, Colloids Surfaces A Physicochem. Eng. Asp. 456 (2014) 129–138, https://doi.org/10.1016/j.colsurfa.2014.05.022.
[63] D. Le Botlan, J. Wennington, J.C. Cheftel, Study of the state of water and oil in frozen emulsions using time domain nmr, J. Colloid Interface Sci. 226 (2000) 16–21, https://doi.org/10.1006/jcis.2000.6785.
[64] V. Krstonošić, L. Dokić, I. Nikolić, M. Milanović, Influence of xanthan gum on oil-in-water emulsion characteristics stabilized by OSA starch, Food Hydrocoll. 45 (2015) 9–17, https://doi.org/10.1016/j.foodhyd.2014.10.024.